Polarization Resolved Laser-Induced Breakdown Spectroscopy of Al[†]

John S. Penczak, Yaoming Liu, and Robert J. Gordon*

Department of Chemistry (m/c 111), University of Illinois at Chicago, Chicago, Illinois 60607

Received: May 20, 2009; Revised Manuscript Received: July 14, 2009

It is shown that the continuous background of the laser-induced breakdown spectrum of Al produced by 800 nm femtosecond pulses is strongly polarized. Use of a polarizer to filter out the background significantly improves the signal/noise and signal/background ratios of the discrete line spectrum. The effects of the laser pulse energy, focal position, incidence and detection angles, and the polarization plane of the laser were investigated. Polarization resolved laser-induced breakdown spectroscopy (PRLIBS) is much less sensitive to these variables than conventional, ungated fs-LIBS, making this a much more versatile analytical tool. These measurements reveal qualitatively different mechanisms for the continuous and discrete parts of the spectrum.

I. Introduction

The technique of laser-induced breakdown spectroscopy (LIBS), also known as laser-induced plasma spectroscopy (LIPS), has become an increasingly important analytical tool since its inception several decades ago.[1,2] The basis for this technology is the observation of fluorescence from a laser-produced plasma. In this respect LIBS can be viewed as a universal sampling, atomization, excitation, and ionization source.[3] LIBS has the advantages of being applicable to solid, liquid, and gas phases as well as being capable of sampling different sections of a material.[4] This highly versatile technique has been applied to such diverse fields as environmental monitoring (e.g., the measurement of greenhouse gases,[5] metallic pollutants,[6] and soil and water contaminants[7]), biomedicine,[8–10] archeology,[11–13] and space exploration.[14,15]

Although LIBS has been successful in numerous applications, it still lacks the sensitivity, accuracy, and precision of other analytical techniques. There have been many studies that attempted to optimize LIBS parameters, but the method is still found to be highly dependent on experimental conditions.[16] Such studies tried to determine the best operating conditions by optimizing parameters such as laser pulse energy, wavelength, pulse duration, and focusing and detection geometries.[17] Although some generalizations can be made from their findings, it is difficult to formulate a complete picture of the optimum conditions for LIBS experiments.

It is generally known that a major limitation to LIBS performance is the production of strong continuum background radiation in the early stages of plasma formation. The main sources of continuum emission are generally believed to be bremsstrahlung and radiative recombination of electrons within the hot dense plasma.[18]

This background interferes with early spectroscopic analysis because it masks the atomic and ionic emission lines. Previous studies showed that the lifetime of the continuum is much shorter than that of the discrete spectrum.[3,17,19,20] A commonly used method of suppressing the background is to detect the plasma emission with an intensified charge-coupled device (ICCD) camera, which can be used to delay and gate the fluorescence measurement, effectively waiting for the continuum background

emission to subside.[2–4,16–19] Although this technique provides good spectra, it does so at great expense and must be optimized for each experimental setup.[17]
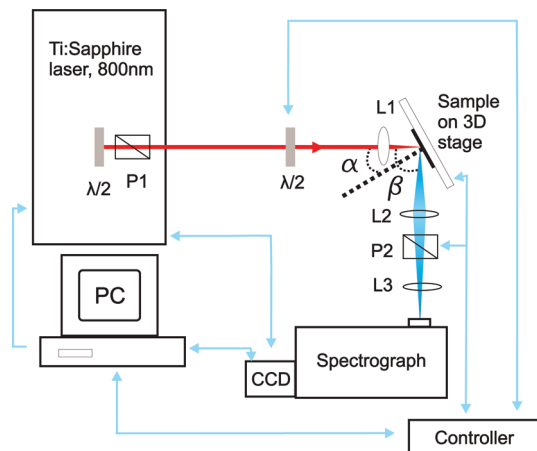
Recently we discovered that the continuum emission produced with fs laser excitation of solid materials may be strongly polarized, while the discrete emission lines are much less polarized.[21] In our initial study we used a pair of laser pulses to ablate Si(111) crystals and observed that the continuum polarization increases with the delay between pulses up to 80 ps. We also found that the amount of polarization increases with decreasing wavelength, exceeding 90% for $\lambda < 350$ nm. With this knowledge, we were able to improve the sensitivity and resolution of LIBS by placing a polarizer before the detector to reduce the continuum emission.[22] We refer to this technique as polarization-resolved LIBS or PRLIBS.

The generation of strongly polarized continuum emission involves a highly directional interaction of electrons with the surrounding medium. The mechanism causing such directionality and the subsequent production of polarized light is of fundamental interest and is the subject of ongoing study. Here we explore in greater detail the experimental conditions that lead to polarized emission, in an attempt to elucidate the key features of PRLIBS as an analytical technique. We use Al as our target material, allowing us to compare the PRLIBS effect with our earlier study of a semiconductor. Also, we limit our study to single pulses, which are more practical for analytical applications.

II. Experimental Section

The apparatus is shown schematically in Figure 1. Single pulses of ~50 fs duration at a central wavelength of 800 nm were generated by a Ti:Sapphire laser (Spectra Physics Tsunami oscillator and Spitfire amplifier). The output of the regenerative amplifier had a contrast ratio of 500 at 13.5 ps and a postpulse pedestal ratio >100 at a time >1 ns away from the main pulse. A half-wave plate and polarizer ($\lambda/2$ and P1 in Figure 1) installed in the amplifier cavity before the compressor were used to reduce the pulse energy to within the range of $10-50\ \mu$J, with a shot-to-shot variation of less than 3%. The beam was focused on the target with a convex lens (L1, $f = 150$ mm). The beam diameter, measured with a scanning knife edge, was ~45 μm, corresponding to a fluence between 0.6 to 3 J/cm^2 at the focal

Laser-Induced Breakdown Spectroscopy of Al

J. Phys. Chem. A, Vol. 113, No. 47, 2009 **13311**

Figure 1. Schematic drawing of the apparatus used, including half-wave plates ($\lambda/2$), polarizers (P1 and P2), and lenses (L1, L2, and L3).
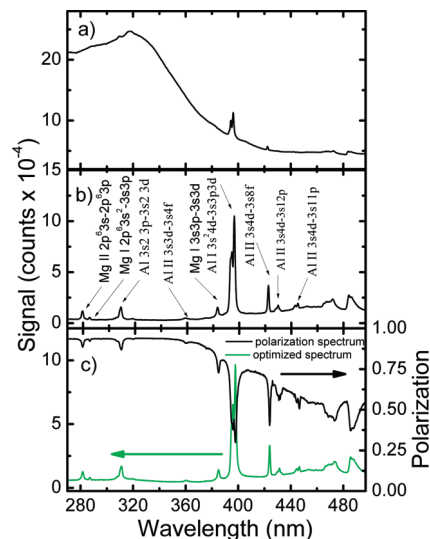

Figure 2. Aluminum spectra recorded with a pulse energy of 50 μJ, s-polarization of the laser, an angle of incidence of $\alpha = 30°$, laser focus on the surface, and the detector positioned perpendicular to the laser beam ($\beta = 90°$). (a) Typical unoptimized LIBS spectrum (recorded without a polarizer) showing large continuum background emission. (b) Fully optimized (PRLIBS) spectrum, recorded with a polarizer placed in front of the detector positioned to reject the polarized background. The two broad unassigned peaks at $\lambda > 460$ nm are from impurities. (c) The top curve is the polarization spectrum showing the degree of polarization measured at each wavelength. The bottom is the same PRLIBS spectrum shown in panel (b). The standard deviations of the points in this and other figures are typically smaller than the size of the symbols.

point. The same knife edge was used to locate the focal point with an accuracy of 13 μm. The Rayleigh range of the focused laser beam was 808 μm.

A hand-polished, industrial grade aluminum alloy sample (either alloy #6061, 97.95% Al, 0.2−1.2% Mg or #7075, 91.0% Al, 6.0% Zn, 2.5% Mg) was mounted on a micrometer-precision *xyz* translation stage (Newport 462 Series) in open air. The stage was computer-controlled to allow the sample to be moved after each laser shot, exposing a fresh surface for each incident pulse. The incident angle of the laser beam and the detection angle were manually adjusted by moving the translation stage or incident laser beam optics. The fluorescence from the plasma plume was focused onto the 50 μm wide slit of a spectrograph (Spectrapro 2300i, Princeton Instruments) with a pair of lenses (L2 and L3) having focal lengths of 50 and 75 mm, respectively. The spectrum was dispersed by a 300 lines/mm grating blazed at 500 nm and was recorded by a nongated thermoelectrically cooled CCD camera (PIXIS 400, Princeton Instruments). Each spectrum is the sum of 20 laser shots, except where noted otherwise.
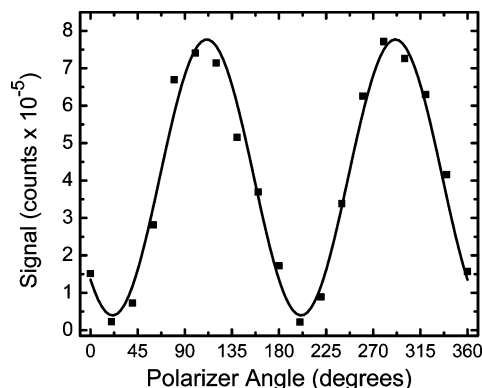
A half-wave plate placed before the focusing lens was used to change the polarization direction of the linearly polarized incident laser. A Glan-Thompson polarizer (P2) was placed in front of the detector between the two focusing lenses. Both the half-wave plate and polarizer were mounted on computer-controlled motorized rotation stages (PR50, Newport). The magnitude of the polarization, *P*, was measured by rotating the polarizer in 20° increments and taking a new spectrum at each spot. The signal was then fit to a Malus law plot of the form of $A + B \cos^2 \theta$, where θ is the angle of the polarizer, yielding $P = B/(2A + B)$.

III. Results

A. Overview. The basic phenomenon of PRLIBS is illustrated in Figure 2. Panel (a) shows the fluorescence spectrum (i.e., the ungated fs-LIBS spectrum) of Al recorded without a polarizer. The spectrum is dominated by a continuum that grows in intensity at shorter wavelengths, with very little discrete structure. Introduction of a polarizer aligned at the angle of minimum transmission eliminates most of the continuum, revealing many atomic and ionic lines (Figure 2b).[23] A typical Malus plot is shown in Figure 3, which was used to determine *P* in 0.2 nm intervals. The resulting polarization spectrum is shown in Figure 2c. A remarkable symmetry between the intensity and polarization spectra is evident, with all the peaks

Figure 3. Typical plot of the emission intensity at a given wavelength recorded at 20° intervals. The data correspond to a wavelength of 245 nm, recorded under the same conditions as Figure 2. The curve is a Malus type function fitted to the data.

in the former appearing as minima in the latter. The comparison of the intensity and polarization spectra is similar to our previously reported data for Si,[21] except that here we obtain greater than 90% polarization at $\lambda < 375$ nm for single pulses.

In the following sections we systematically explore the effects of laser pulse energy, focal position, incidence and detection angles, and polarization plane. The "standard" experimental conditions used throughout were 50 μJ (corresponding to a fluence of 3.1 J/cm^2 and an intensity of 6.2×10^{13} W/cm^2) of s-polarized radiation focused on the target surface, at a 30° angle of incidence with respect to the normal, with the detector located in the plane of incidence, perpendicular to the laser beam. Individual parameters were varied for specific experiments, *mutatis mutandis,* as indicated in each section.

B. Pulse Energy. In Figure 4a, the LIBS spectra of Al are shown for pulse energies of 12.5, 25, and 50 μJ (measured
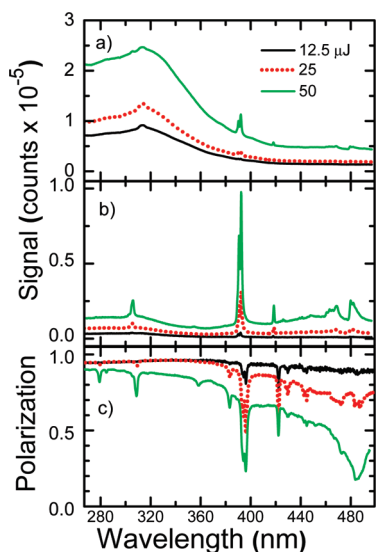
Figure 4. Effect of the laser pulse energy, taken under the same conditions as Figure 2, but with pulse energies of 12.5, 25, and 50 μJ. (a) Unoptimized LIBS spectra (taken without the polarizer); (b) PRLIBS spectra taken with the polarizer in place; (c) polarization spectra.

without a polarizer). It is apparent that the signal intensity increases with pulse energy. This behavior is consistent with previous findings that an increase in pulse energy produces a higher LIBS signal and larger ablated crater volume.[24,25] This result has been found for different fluence regimes and pulse durations.[2,17,21,26–28] The reason for this behavior may be related to the lifetime of the plasma, which has also been found to increase with pulse energy,[7] as well as to larger concentrations of excited species. Both the continuum and the discrete lines grow with pulse energy. Especially at low energy, there is a noticeable loss of information in the spectra caused by the continuum background.

In Figure 4b the same experiment was performed, but the spectra were collected with the aid of a polarizer that was rotated to block out the polarized emission. The discrete lines, being much less polarized, are less affected by the polarizer and therefore grow relative to the background. This enhancement is particularly evident for the Al peak at 309 nm, the doublet peak at 394 and 396 nm, and the peak at 422 nm. The improvements in the signal-to-noise (S/N) and signal-to-background (S/B) ratios at 396 nm are listed in Table 1. Without the polarizer, S/N (defined as the peak height divided by the rms variation of the adjacent background) lies in the range of ~40–60, whereas S/B (defined as signal + background divided by the adjacent background) grows from 1.1 to 1.5. Inserting the polarizer increases S/B by 10-fold at all energies. The S/N ratios increase by a factor of ~4, except at the lowest energy where it decreases by about 50%. This last effect may be attributed to the fact that at very low energies the signal is very weak, and its attenuation by the polarizer is not accompanied by a corresponding reduction of the background.

Figure 4c shows the polarization as a function of wavelength at different energies. We find that P decreases with increasing pulse energy. At the lowest energy the signal is nearly totally polarized, an observation that is consistent with the featureless spectrum in Figure 4a. It is also shown that the discrete lines appear as dips in the polarization spectrum, which explains why they are less affected by the polarizer. Even as the polarization tapers off at longer wavelengths, the effect of the polarizer is significant.

C. Focal Position. A systematic study of the focal position was conducted by first finding the minimum spot size with the aid of the scanning knife-edge. Spectra were then recorded at 0.1 mm increments in focal position, above, below and on the target surface. This process was carried out until there was a significant loss of spectral intensity. At higher pulse energies we were able to bring the laser further out of focus and still obtain spectra resembling those obtained at lower energies closer to the surface. This observation suggests that the dependence of the spectra on focal position is determined more by fluence than pulse energy.

Three representative spectra are shown in Figure 5a. We find that without a polarizer the maximum S/N and S/B are obtained for a focus ~0.25 mm beneath the surface (see Figure 6). The most intense signals, however, were obtained with the focus above and further below the surface. Our observations are consistent with previous studies using ns lasers, which also obtained the best signal quality by focusing beneath the surface. The deterioration of signal quality for above-surface focusing is generally attributed to shielding of the laser pulse by a plasma produced by air breakdown above the surface.[29–31] This explanation could apply here as well, and should be distinguished from shielding by the ablation-generated plasma, which does not occur on the time scale of the fs laser pulse. We note that a study comparing ns- and fs-LIBS[19] obtained optimum signals for focusing above the surface. It is likely that the much lower ambient pressures used in that study reduced the effects of above-surface breakdown.

Interestingly, we find that not only the intensity but also the structure of the spectrum is affected by the focal position, although a consistent correlation between spectral features and focal position was not obtained. The shapes of both the continuum emission as well as that of some of the peaks are appreciably affected by the focal position. For example, for a focal point beneath the surface, the background tends to extend throughout most of the wavelength range but still supports some discrete structure. As evident in Figure 5a, the structure is not symmetric with respect to the location of the focal point above and below the surface, and the loss of structure is not uniform across the spectrum. We find a considerably more pronounced continuum in the short wavelength range (<340 nm), where the peaks at 278 and 308 nm are obscured, whereas the spectra at longer wavelengths more closely resemble the on-focus spectrum.

The effects of the focal position are largely offset by using a polarizer to filter out the continuum. As shown in Figure 5b, spectra taken with the polarizer angle set for minimum transmission show an order of magnitude decrease in continuum emission at all wavelengths, whereas the peaks suffer only ~3-fold decrease. The overall result is a 3–4-fold increase in S/B and a 20–100% increase in S/N, as shown in Figure 6. The largest S/N is obtained on focus and the largest S/B is obtained 0.5 mm above the surface.

It is important to note that the polarizer not only increases the S/N and S/B ratios but also reduces their sensitivity to focal position. Inspection of Figure 5b shows that the PRLIBS spectra taken with the focus above, below, and on the surface are very similar. In Figure 5c we see that the polarization spectra are also similar, differing mainly in the amount of polarization. For the on-focus case, the fluence at the sample surface is greatest and P is smallest. This result is consistent with our finding in Figure 4c that P decreases with increasing fluence. Figure 5c also shows that the highest P is obtained for above-surface focusing, which is consistent with the maximum S/B found there. The mechanism for this increased polarization is as yet

Laser-Induced Breakdown Spectroscopy of Al

J. Phys. Chem. A, Vol. 113, No. 47, 2009 **13313**

TABLE 1: Signal to Noise (S/N) and Signal to Background (S/B) Ratios at 396.15 nm

observable	pulse energy (μJ)			angle of incidence			detector angle			
	12.5	25	50	0	30	45	45	60	75	90
S/N w/o polarizer	38	39	61	293	143	47	107	110	101	151
S/N with polarizer	17	127	222	452	194	266	128	281	339	387
S/B w/o polarizer	1.1	1.2	1.5	11.7	4.4	1.5	1.3	1.1	1.3	1.6
S/B with polarizer	8.2	13.2	10.8	16.4	11.2	9.8	11.6	6.1	14.8	9.2

undetermined. It is evident that since the structure of the polarization spectrum is insensitive to focal position, both the polarization and the PRLIBS spectra offer greater sensitivity and resolution than conventional ungated fs-LIBS spectra. Filtering out the polarized background lends greater flexibility to the PRLIBS technique, allowing for a much wider range of sample positions or surface roughness, with a much weaker dependence on the focal point.
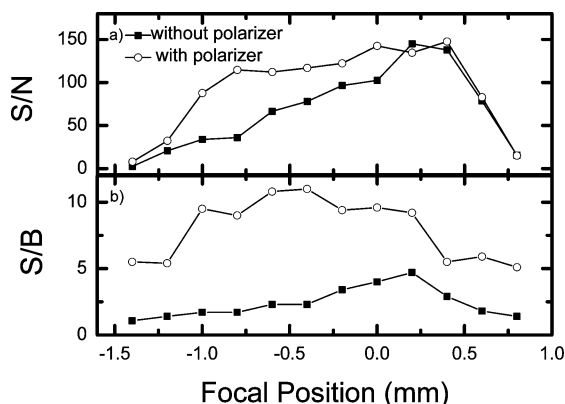
D. Angle of Incidence. When an intense laser strikes a metal surface, it produces an overdense plasma within a few optical cycles.[32] This surface plasma should not be confused with the underdense plasma that evolves on a much longer time scale

Figure 5. Effect of laser focal position, taken under the same conditions as Figure 2 but with the laser focused at different depths; $z < 0$ corresponds to a focal point above the surface, and $z > 0$ is for the focal point beneath the surface. (a) Unoptimized LIBS spectra (taken without the polarizer); (b) PRLIBS spectra taken with the polarizer in place; (c) polarization spectra.

Figure 6. Signal to noise ratio (a) and signal to background ratio (b) at 396.15 nm, measured with and without the polarizer in place at varying focal positions. Experimental conditions are the same as in Figure 5.

above the surface and shields it from the tail of a long laser pulse. It is well-known that the strength of the laser−surface interaction is sensitive to the angle of incidence, α.[33] As a practical matter, it is not always possible to select α when using LIBS for standoff material analysis.
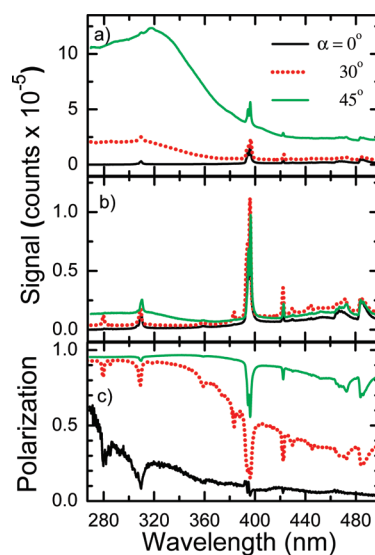
In Figure 7, three values of α were employed: $\alpha = 0°$ (normal incidence), 30° and 45°. In each case the detector was placed normal to the laser, which means that for $\alpha = 0$ the line-of-sight was parallel to the target surface, and for $\alpha = 45°$ the detector was placed at the specular angle. We find that the spectrum without a polarizer (Figure 7a) is very sensitive to α. At normal incidence the continuum emission almost completely disappears, producing S/N and S/B ratios that are comparable to those obtained in experiments using the polarizer to reduce the continuum emission. The effect is consistent with the polarization spectrum (Figure 7c), which shows considerably less polarization at normal incidence than at other incident angles. For oblique angles of incidence, the continuum emission appears to increase nonlinearly with α. The intensity of the continuum emission in Figure 7a follows the same trend as the magnitude of the polarization in Figure 7c, with $P > 0.7$ over the entire spectral range of the continuum for $\alpha = 45°$. The S/N and S/B ratios without a polarizer in Table 1 follow the same trend as the polarization and continuum emission intensities, falling off sharply with increasing α. Again, the polarizer was employed to resolve the peaks in the LIBS spectra, as shown in Figure 7b. The fractional improvement in S/B and S/N ratios increases with α, and even at normal incidence these ratios are improved by ~50%. We observe that the polarizer is unable

Figure 7. Effect of the angle of incidence, α, measured with respect to the surface normal. The experimental conditions are the same as in Figure 2, except that α has values of 0° (normal incidence), 30° and 45°. The uncertainty in α is ±3°. The detector is always normal to the laser direction. (a) Unoptimized LIBS spectra (taken without the polarizer); (b) PRLIBS spectra taken with the polarizer in place; (c) polarization spectra.

13314 *J. Phys. Chem. A, Vol. 113, No. 47, 2009*

Penczak et al.
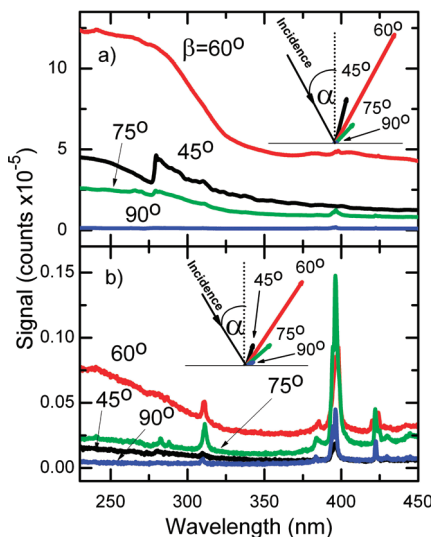
Figure 8. Effect of the detector angle, β, measured with respect to the direction of the laser on (a) the unoptimized LIBS spectra (taken without the polarizer) and (b) the PRLIBS spectra taken with the polarizer in place. The experimental conditions are the same as in Figure 2, except that β has values of 45°, 60°, 75°, and 90°, and the pulse energy is 25 μJ. The uncertainty in β is $\pm$3°. The inset in each panel is a polar plot of the signal at 230 nm.

completely to resolve the spectra taken at $\alpha = 45$°, and some of the peaks at shorter wavelengths are obscured. The polarization spectrum shows that the emission is ~95% polarized in this region. For this angle of incidence some of the discrete lines do not appear in the polarization spectrum, possibly because they are more strongly polarized than at the other two angles of incidence.

In changing the angle of incidence we simultaneously change the laser fluence and surface reflectance. As α increases, the fluence decreases and the Fresnel reflectance of s-polarized light increases.[34] In going from $\alpha = 0$° to $\alpha = 45$° the fluence drops by a factor of 2, and the reflectance (obtained from a Drude$-$Fresnel model) increases by ~15%.[35] Surprisingly, the continuum signal increases with α, despite the lower fluence and reduced absorbance, whereas the discrete signal is roughly independent of angle. As shown in the following section, the continuum behavior may be explained in part by the restricted detection angle.

E. Detection Angle. The angular distribution of the plasma emission is likely to provide valuable clues to the mechanism that produces the polarized emission. As in the case of α, it is not always practical to select the detection angle, β, which is defined with respect to the laser direction (see Figure 1). Accurate measurements of the effects of varying β were more difficult to obtain because the detector had to be moved physically for each change in angle. The spectra shown in Figure 8 were obtained with $\alpha = 30$° and a pulse energy of 25 μJ. The more intense spectra were found to be saturated at higher energy.

Figure 8a shows the LIBS spectrum recorded without a polarizer, and Figure 8b shows the PRLIBS spectrum with the polarizer set for minimum transmission. The spectra, in order of decreasing intensity, were recorded at $\beta = 60$°, 45°, 75°, and 90°.[36] At first glance the intensity sequence is puzzling, but when plotted in polar form (see insets in Figure 8) at a specific continuum wavelength (230 nm), it becomes evident that the emission is highly directional, with a peak at the specular angle ($\beta = 60$°). This finding explains the anomalies reported in the previous section. The maximum intensity was observed
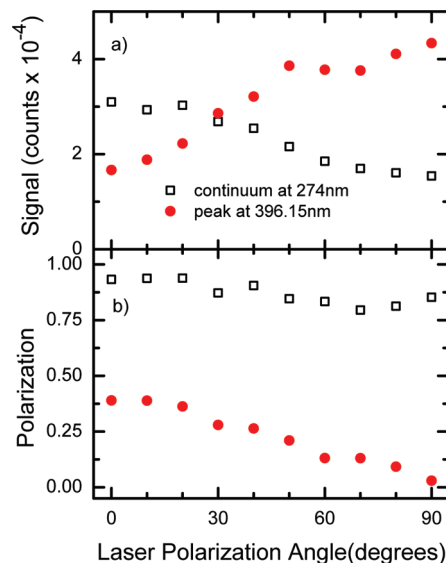
Figure 9. Effect of the direction of the laser polarization on the intensity (a) and degree of polarization (b). An angle of 0° corresponds to s-polarization, and 90° corresponds to p-polarization. Solid symbols correspond to discrete emission at 396.15 nm, and open symbols correspond to continuum emission measured at 274 nm. All other conditions are the same as in Figure 2. The points are averages of 200 laser shots.

at $\alpha = 45$° because the detector was at the specular angle ($\beta = 45$°), whereas almost no continuum was observed for $\alpha = 0$° because the detector was normal to the specular angle. We also find that the width of the angular distribution of the continuum is sensitive to the focal position. Although the LIBS spectra near the specular angle are almost completely featureless, insertion of the polarizer restores the discrete structure.

F. Laser Polarization. All the spectra reported hitherto were recorded with an s-polarized laser (polarization perpendicular to the plane of incidence). In Figure 9 we explore the effect of rotating the laser polarization from s to p. Figure 9a shows that the intensity of the continuum (measured at 274 nm) decreases by 50% as the laser polarization is rotated, while the intensity of the discrete emission (measured at 396.15 nm) increases by a factor of 2.5. The continuum was measured here without a polarizer, while the discrete peak was measured with the polarizer set to reject the contribution from the continuum. Figure 9b shows the variation in P with laser polarization. We find that a small (~10%) but reproducible drop in the polarization of the continuum as the laser polarization is changed from s to p. This trend is consistent with the decrease in the projection of the electric field parallel to the surface as the laser polarization changes from s to p, but other factors may be involved as well. A much more dramatic falloff of the polarization is observed for the discrete emission. It is difficult to determine from the present data whether this falloff is due to a change in the value of P for the discrete emission or to variation in the relative intensities of the discrete vs continuum emission as a function of laser polarization angle. A consistent interpretation of the data is that the discrete emission is weakly polarized and the intensity of that emission (i.e., the concentration of emitting species) increases as the laser polarization is changed from s to p.

IV. Discussion

There is ample experimental evidence pointing to very different mechanisms for the discrete and continuous emission.

Laser-Induced Breakdown Spectroscopy of Al

J. Phys. Chem. A, Vol. 113, No. 47, 2009 **13315**

The most dramatic example is a comparison of the emission and polarization spectra shown in Figure 2c. These spectra are nearly mirror images of each other, with each peak in the PRLIBS spectrum appearing as a window in the polarization spectrum. These spectra show that discrete peaks are much less polarized than the background. Second, we observe in Figure 9a opposite dependences of the intensities of the discrete and continuum spectra on laser polarization, with the former more intense for p-polarization and the latter more intense for s-polarization. A third point is the fluorescence lifetime. Previous studies showed, and our own measurements confirm,[37] that the continuum is much shorter lived than the discrete emission. Fourth, we find that the continuum is directional with a maximum at the specular angle, whereas the discrete emission has little or no directionality. Conventional LIBS measurements use time gating to suppress the continuum. Here we have shown that the polarization and directionality of the continuum emission provide two additional methods of increasing the S/B ratio.

A number of previous studies revealed various degrees of polarization of the discrete emission. X-rays emitted by plasmas generated with ultraintense lasers have been found to be polarized,[38,39] and values of $P > 50\%$ has been reported.[40] Laser-generated plasma polarization has been observed also under much milder conditions. J. Kim and D. E. Kim[41] observed discrete line emission from Al III produced by irradiation of an Al crystal in air with 3 ns, 1064 nm pulses. They reported a maximum polarization of 2.1%, which decreased with the distance of the focal point from the surface. Kim and Lee[42] used 25 ns, 1064 nm pulses to study the spatial distribution of the plasma emission from Al. They observed a complex pattern, with localized regions of very high polarization and others with zero polarization. Sharma and Thareja[43] measured the polarization of Al III produced by 35 ps, 1064 nm pulses as a function of time after the pulse, both in vacuum and up to 70 Torr of ambient N_2. They observed P as large as 30% after a delay greater than 100 ns. More recently[44] they studied the same system using 8 ns, 1064 nm pulses. For pressures ≥ 0.1 Torr, P was generally small; however, large polarization was observed under vacuum at delays around 200 ns. None of these studies systematically compared the polarization of the discrete spectrum with that of the continuum, and it is possible that part of the reported polarization was caused by the underlying continuum.

The discrete emission results from radiative decay of electronically excited atoms and ions present in the laser-generated plasma. Polarized emission in such transitions results from a nonstatistical distribution of magnetic substates.[45] The nonstatistical distribution could be a property of the nascent atoms or ions produced by laser ablation of the aluminum target or be produced by electron bombardment of these species in the plasma. The magnitude of the polarization is related to the alignment parameter, A_L, given by[46]

$$A_L(p \rightarrow s) = \frac{2P}{3 - P} = (-1)^{J_p + J_s} \sqrt{3/2}(2J_p + 1) \times$$
$$\begin{Bmatrix} J_p & J_p & 2 \\ 1 & 1 & J_s \end{Bmatrix} \frac{a(p)}{n(p)} \quad (1)$$

where J_p and J_s are the total angular momentum quantum numbers of the upper and lower states, the bracket is a 6j symbol, $a(p)$ is the alignment of the sublevels of the upper state, and $n(p)$ is their population. (The labels p and s used here should not be confused with the polarization state of the laser.) The 6j symbol varies strongly from state to state and can be both

positive and negative. Our observation that the polarization of the discrete emission appears as minima with respect to the continuum implies that its value must be much smaller than that of the continuum. Large nascent values of $a(p)$ could result from excitation of atoms and ions by electrons having an anisotropic velocity distribution. The small values of $|a(p)|$ present here are readily explained by the many collisions that occur with atmospheric molecules during the radiative lifetime of the excited states. In future experiments we plan to measure P as a function of ambient pressure.

Continuum emission is produced by free−free (bremsstrahlung) and bound−free (recombination) transitions of electrons in a plasma.[47] More complex processes could occur in the laser−surface interaction.[32] We will use electron recombination to illustrate how the polarized continuum might be produced, although in reality the mechanism could be much more complex. Recombination of an electron with an ion of charge $+z$,

$$e^- + M^{+z} \rightarrow M^{+(z-1)}(\Gamma) + \hbar\omega \quad (2)$$
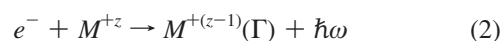
yields an atom or ion $M^{+(z-1)}$ in electronically excited state Γ and a photon of frequency ω.[48] The continuous energy of the photon is given by

$$\hbar\omega = E + \chi_\Gamma, \quad (3)$$

where E is the kinetic energy of the electron, and χ_Γ is the binding energy of state Γ. The polarization of the photon is determined by the anisotropy of the velocity distribution of the recombining electrons. The reverse of process 2 is photoionization, for which the differential cross section in the dipole approximation is proportional to $1 + \beta_\Gamma P_2(\hat{v} \cdot \hat{\varepsilon})$, where $\hat{\varepsilon}$ is the polarization vector of the absorbed photon, $\hat{v}$ is the velocity direction of the emitted electrons, P_2 is the second order Legendre polynomial, and the anisotropy parameter has values $-1 \leq \beta_\Gamma \leq 2$.[49] Milchberg and Weisheit[50] (MW) used detailed balancing to apply this cross section to determine the polarization of the outgoing photon produced by electron recombination. Expanding the anisotropic velocity distribution of the electrons in a Legendre series,

$$f(\vec{v}) = \sum_{n=0}^{\infty} f_n(v) P_n(\cos\theta), \qquad \theta = \hat{v} \cdot \hat{\varepsilon} \quad (4)$$

they showed that the maximum observable polarization is given by

$$P = \frac{3\beta_\Gamma f_2(v)}{20f_0(v) + \beta_\Gamma f_2(v)} \quad (5)$$

We see that the polarization depends on the electronic properties of the recombined state and the quadrupole moment of the electron velocity distribution. Although neither can be determined from the present data, we are able to explain several qualitative properties of the polarization spectrum. Consider the model case of a bi-Maxwellian velocity distribution with a constant axial drift,[50]

13316 *J. Phys. Chem. A, Vol. 113, No. 47, 2009*

Penczak et al.

$$f(\vec{v}) \propto \exp\left\{-\frac{m_e v^2 \sin^2\theta}{2kT_\perp} - \frac{m_e(v\cos\theta - u_D)^2}{2kT_\parallel}\right\} \quad (6)$$

where $T_\parallel$ and $T_\perp$ are the axial and transverse temperatures, m_e is the electron mass, and u_D is the drift velocity. This distribution function is characterized by two dimensionless quantities,

$$\xi = \left(\frac{E}{kT_\parallel}\right)(1 - T_\parallel/T_\perp) \approx -\frac{E}{kT_\perp}, \qquad T_\parallel \gg T_\perp \quad (7)$$

and

$$\Lambda = \frac{\sqrt{2m_e E}u_D}{kT_\parallel} \quad (8)$$

MW showed that for $\Lambda = 0$, P increases monotonically with $\xi \to -\infty$, reaching an asymptotic value of $3\beta_\Gamma/(8 - \beta_\Gamma)$, whereas for $\xi = 0$, P increases monotonically with increasing Λ, reaching an asymptotic value of $3\beta_\Gamma/(4 + \beta_\Gamma)$. Both limits give $P = 1$ for $\beta_\Gamma = 2$, which corresponds to Γ being an S state. The increase of P with photon frequency is simply a consequence of the increased kinetic energy of the recombining electrons in eqs 2, 6, and 7. Although it seems unlikely that only S states are formed, Kim and Pratt[51] showed that low orbital angular momentum states are preferred. Whereas this kind of analysis is more typically used to characterize the velocity distributions of electrons with keV energies, which recombine or undergo bremsstrahlung interactions to emit X-radiation,[52] it could apply also to the much lower (2−5 eV) continuum energies observed here. An explanation of our finding of nearly total polarization probably requires going beyond the assumptions of the dipole approximation and Maxwellian distributions, and needs to take into account the effects of electric and magnetic fields generated in the plasma.

While the broad outline of the PRLIBS effect may be understood in terms of the mechanisms described above, many of the detailed results require further study. The different polarization of the discrete and continuous spectra in Figure 2 may be explained by the collisional quenching rates of the emitting species. We know that the atoms and ions emitting the discrete lines undergo many collisions during their lifetimes, whereas previous work[3,17,19,20] shows that the emission rate of the continuum is greater than the electron quenching rate. The specific mechanism responsible for generating the excited species, and, in particular, the origin of the anisotropy that is ultimately responsible for the photon polarization, is unknown. The preference for p-polarized laser excitation (Figure 9a) for the discrete emission is consistent with resonance excitation of the surface plasma produced during the early part of the laser pulse.[33,53] The sizable emission produced with s-polarization and the insensitivity of the signal to incidence angle, however, indicate a more complex mechanism. The decline in the polarization of the discrete lines as the laser polarization is changed from s to p (Figure 9b) may simply reflect the fact that discrete line emission is a larger fraction of the total signal as the polarization becomes more p-like. The apparent independence of the discrete signal on angle of incidence may be due to a cancellation of opposite effects (stronger absorption of p-polarized radiation at oblique angles vs decreasing fluence as α is increased).

The properties of the continuum emission are more difficult to explain. Collisional plasma excitation is consistent with s-polarization,[33] but the polarization and angular distributions are unexplained at this point. The decrease of P with increasing pulse energy (Figure 4c) could be explained by the hotter plasma being more isotropic. This effect would appear as an increase in temperatures $T_\parallel$ and $T_\perp$ in eqs 6 and 7.

In summary, we have systematically studied the properties of the polarized plasma emission generated by the ablation of an Al target in air with femtosecond laser pulses. As in our previous study of Si,[21] we observed that the continuum emission is nearly totally polarized, while discrete line emission appears as minima in the polarization spectrum. In contrast to the previous study, very large polarizations were obtained with single (as opposed to double) pulses. The discrete line intensity for p-polarized excitation is 2.5 times larger than that for s-polarized excitation, which is consistent with resonance absorption by the surface plasma. The intensity and degree of polarization of the continuum decrease slowly as the laser polarization is changed from s to p. We also find that the continuum emission is strongly peaked at the specular angle. Polarization resolved LIBS (PRLIBS) may be valuable as an analytical tool because it is much less sensitive to laser and detector properties as compared with conventional ungated LIBS.

References and Notes

(1) Singh, J. P.; Thakur, S. N. *Laser-Induced Breakdown Spectroscopy*; Elsevier: Boston, 2007.

(2) Sirven, J.; Mauchien, P.; Sallé, B. *Spectrochim. Acta, Part B* **2008**, *63*, 1077.

(3) Le Drogoff, B.; Margo, J.; Chaker, M.; Sabsabi, M.; Barthelemy, O.; Johnston, T. W.; Laville, S.; Vidal, F.; von Kaenel, Y. *Spectrochim. Acta, Part B* **2001**, *56*, 987.

(4) Rohwetter, P.; Yu, J.; Mejean, G.; Stelmaszczyk, K.; Salmon, E.; Kasparian, J.; Wolf, J. P.; Wõstea, L. *J. Anal. At. Spectrom.* **2004**, *19*, 437.

(5) Williamson, C. K.; Daniel, R. G.; McNesby, K. L.; Miziolek, A. W. *Anal. Chem.* **1998**, *70*, 1186.

(6) Wainner, R. T.; Harmon, R. S.; Miziolek, A. W.; McNesby, K. L.; French, P. D. *Spectrochim. Acta, Part B* **2001**, *56*, 777.

(7) Lazic, V.; Barbini, R.; Colao, F.; Fantoni, R.; Palucci, A. *Spectrochim. Acta, Part B* **2002**, *56* (6), 807.

(8) Serbin, J.; Bauer, T.; Fallnich, C. *Appl. Surf. Sci.* **2002**, *197*, 737.

(9) Lubatschowski, H.; Maatz, G.; Heisterkamp, A. *Graefe's Arch. Clin. Exp. Ophthalmol.* **2000**, *238*, 33.

(10) Diedrich, J.; Rehse, S. J.; Palchaudhuri, S. *J. Appl. Phys.* **2007**, *102*, 014702.

(11) Giakoumaki, A.; Melessanaki, K.; Anglos, D. *Anal. Bioanal. Chem.* **2007**, *387*, 749.

(12) Brysbaert, A.; Melessanaki, K.; Anglos, D. *J. Arch. Sci.* **2006**, *33*, 1095.

(13) Melessanaki, K.; Mateo, M.; Ferrence, S. C. *Appl. Surf. Sci.* **2002**, *197*, 156.

(14) Salle, B.; Cremers, D. A.; Maurice, S. *Spectrochim. Acta, Part B* **2005**, *60*, 479.

(15) Arp, Z. A.; Cremers, D. A.; Wiens, R. C. *Appl. Spectrosc.* **2004**, *58*, 897.

(16) Elhassan, A.; Giakoumaki, A.; Anglos, D.; Ingo, G. M.; Robbiola, L.; Harith, M. A. *Spectrochim. Acta, Part B* **2008**, *63*, 504.

(17) Rieger, G. W.; Taschuk, M.; Tsui, Y. Y.; Fedosejevs, R. *Spectrochim. Acta, Part B* **2003**, *58*, 497.

(18) Le Drogoff, B.; Margot, J.; Vidal, F.; Laville, S.; Chaker, M.; Sabsabi, M.; Johnston, T. W.; Barthelemy, O. *Plasma Sources Sci. Technol.* **2004**, *13*, 223.

(19) Margetic, V.; Pakulev1, A.; Stockhaus, A.; Bolshov, M.; Niemax, K.; Hergenroder, U. R. *Spectrochim. Acta, Part B* **2000**, *55*, 1771.

(20) Hohreiter, V.; Hahn, D. W. *Anal. Chem.* **2006**, *78*, 1509.

(21) Liu, Y.; Singha, S.; Witt, T. E.; Cheng, Y.; Gordon, R. J. *Appl. Phys. Lett.* **2008**, *93*, 161502.

(22) Zhao, Y.; Singha, S.; Liu, Y.; et al. *Opt. Lett.* **2009**, *34*, 494.

Laser-Induced Breakdown Spectroscopy of Al

J. Phys. Chem. A, Vol. 113, No. 47, 2009 **13317**

(23) The NIST Chemistry Webbook, http://webbook.nist.gov/chemistry.

(24) Hu, Z.; Singha, S.; Liu, Y.; Gordon, R. J. *Appl. Phys. Lett.* **2007**, *90*, 131910.

(25) Singha, S.; Hu, Z.; Gordon, R. J. *J. Appl. Phys.* **2008**, *104*, 113520.

(26) Schill, A. W.; Heaps, D. A.; Stratis-Cullum, D. N. *Opt. Express* **2007**, *15* (21), 14045.

(27) Sirven, J.-B.; Bousquet, B.; Canioni, L.; Sarger, L. *Spectrochim. Acta, Part B* **2004**, *59*, 1033.

(28) Cravetchi, I. V.; Taschuk, M. T.; Tsui, Y. Y.; Fedosejevs, R. *Anal. Bioanal. Chem.* **2006**, *385*, 287.

(29) Tognoni, E.; Palleschi, V.; Corsi, M.; Cristoforetti, G. *Spectrochim. Acta, Part B* **2002**, *57*, 1115.

(30) Gornushkin, I. B.; et al. *Spectrochim. Acta, Part B* **2004**, *59*, 401.

(31) Barnett, C.; Cahoonª, E.; Almirall, J. R. *Spectrochim. Acta, Part B* **2008**, *63*, 1016.

(32) Gibbon, P. *Short-Pulse Laser Interactions with Matter*; Imperial College Press: London, 2005.

(33) Kruer, W. M. *The Physics of Laser Plasma Interactions*; Westview Press: Boulder, 2003.

(34) Godwin, R. P. *Appl. Opt.* **1994**, *33*, 1063.

(35) Fedosejevs, R.; et al. *Phys. Rev. Lett.* **1990**, *64*, 1250.

(36) The step in the LIBS spectrum at 275 nm measured at $\beta = 45°$ is sensitive to the focal position of the laser. Although reproducible, its cause is unknown.

(37) Details will be reported in a future publication.

(38) Nishimura, H.; et al. *Plasma Phys. Controlled Fusion* **2005**, *47*, B823.

(39) Inubushi, Y.; et al. *Rev. Sci. Instrum.* **2004**, *75*, 3699.

(40) Kawamura, T.; et al. *Phys. Rev. Lett.* **2007**, *99*, 115003.

(41) Kim, J.; Kim, D. *Appl. Surf. Sci.* **2002**, *197\198*, 188.

(42) Kim, Y. W.; Lee, H. D. *Rev. Sci. Instrum.* **2003**, *74*, 2123.

(43) Sharma, A. K.; Thareja, R. K. *J. Appl. Phys.* **2005**, *98*, 033304.

(44) Sharma, A. K.; Thareja, R. K. *Appl. Surf. Sci.* **2007**, *253*, 3113.

(45) Hakel, P.; et al. *Phys. Rev. A* **2007**, *76*, 012716.

(46) Fujimoto, T.; Kazantsev, S. A. *Plasma Phys. Controlled Fusion* **1997**, *39*, 1267.

(47) Fujimoto, T., Iwamae, A., Eds. *Plasma Polarization Spectroscopy*; Springer: Berlin, 2007.

(48) Fujimoto, T. *Plasma Spectroscopy*; Oxford University Press: Oxford, 2004.

(49) Cooper, J.; Zare, R. N. In *Lectures in Theoretical Physics*; Geltman, S., Mahanthappa, K. T., Britten, W. E., Eds.; Gordon and Breach: New York, 1969; p 317.

(50) Milchberg, H. M.; Weisheit, J. C. *Phys. Rev. A* **1982**, *26*, 1023.

(51) Kim, Y. S.; Pratt, R. H. *Phys. Rev. A* **1983**, *27*, 2913.

(52) Lamoureux, M.; Jacquet, L.; Pratt, R. H. *Phys. Rev. A* **1989**, *39*, 6323.

(53) Baldis, H. A.; Campell, E. M.; Kruer, W. L. *Handbook of Plasma Physics*; Rosenbluth, M. N., Sagdeev, R. Z., Eds.; Elsevier: Amsterdam, 1991; Vol. 3.